ACS OMEGA

Open Access

http://pubs.acs.org/journal/acsodf

Article

Study on Green Nanofluid Profile Control and Displacement of Oil in a Low Permeability Reservoir

Yi Shen, Jingchun Wu,* Fang Shi,* Yingwei He, Hongjun Li, Wenxiu Zhou, Manyong Zhao, Chenying Wang, Ying Yan, Mingzheng Lu, Jisheng Ma, and Lili Zheng

Cite This: *ACS Omega* 2023, 8, 38926−38932

Read Online

ACCESS | Metrics & More | Article Recommendations

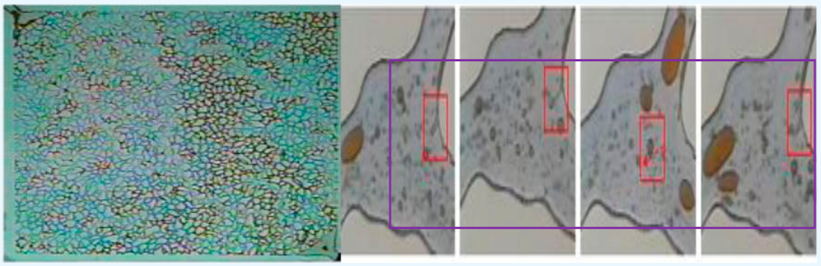

ABSTRACT: Low permeability reservoirs are characterized by low permeability, small pore throat, strong heterogeneity, and poor injection-production ability. High shale content of the reservoir, strong pressure sensitivity, micropore undersaturation, and significant water-lock effect in water injection development lead to increased fluid seepage resistance. There is an urgent need to adopt physical and chemical methods to supplement energy and improve infiltration efficiency, thereby forming effective methods for increasing the production and efficiency. Aiming at the characteristics of ultralow permeability reservoirs, in this paper, a green and environmental friendly biobased profile control and displacement agent (Bio Nano30) has been developed using noncovalent supramolecular interaction. Physical simulation experiments illustrate the profile control and displacement mechanism of Bio-Nano30. Laboratory experiments and field applications show that good results have been achieved in oil well plugging removal, water well pressure reduction and injection increase, and well group profile control and oil displacement. This research has good application prospects in low permeability heterogeneous reservoirs.

1. INTRODUCTION

The reservoir developed by water injection is a huge physical and chemical reactor. The adverse effects of foreign fluids entering the reservoir are essentially the result of various physical processes and chemical reactions between foreign fluids and reservoir fluids or between both and rocks,[1,2] resulting in a decrease in porosity and permeability. Foreign liquids or solids intrude into the oil layer, causing physical and chemical interactions with clay or other sensitive components in the oil layer, resulting in changes in the rock structure, surface properties, mineral composition and properties, and liquid phase state of the oil layer.[3−5] Physical parameters such as porosity, permeability, oil−water saturation, and wettability of the reservoir are changed, thereby reducing the percolation ability of the fluid.[6]

The development of low permeability oil fields usually adopts traditional water injection process, and the main contradictions faced are high water injection pressure, poor efficiency, and low degree of reservoir production.[7−11] Aiming at the problems existing in the development of ultralow permeability reservoirs, studying how to reduce the starting pressure of low permeability reservoirs, improve the development effect of water injection agents, and further improve the recovery efficiency of low permeability oilfields will have very important value for improving the development theory and actual development effect of ultralow permeability oilfields.[12−16] In the practice of water flooding to develop low permeability reservoirs, a lot of detailed research and practical work have been done, such as strengthening water injection with high injection-production ratio in the early stage and restoring formation pressure.[17−20] Early layered water injection was used to control water cut rise. Comprehensive measures have been taken such as plugging, shutting down, and turning over water wells with high water content. These technical measures have achieved certain results, such as conducting secondary and tertiary fracturing transformation in the block to induce efficiency and bring into play the production capacity of

Received: May 6, 2023
Accepted: September 29, 2023
Published: October 13, 2023

Table 1. Constitute Simulation of Formation Water

composition	$Na^+ + K^+$	Ca^{2+}	Mg^{2+}	HCO_3^-	SO_4^{2-}	Cl^-	simulate the mineralization degree
content (mg/L)	1450	15	44	1351	51	1545	4456

oil wells.[21−27] However, many problems have also been exposed during the production, such as low production capacity after the oil well is put into production, and many blocks have no production recovery period. Some oil wells have experienced a rapid increase in water production and a decline in oil well productivity.[28−30] In addition, some oil wells have poor fluid supply capacity, resulting in an increase in nonproduction and low production and efficiency wells. The main measures for increasing crude oil production in oilfields, fracturing measures have less room for tapping potential, and their oil-increasing effects are becoming worse and worse.

In the case of ultralow permeability, the injection system has a slow flow rate, difficult water injection development, difficult starting of crude oil, high start-up pressure, and severe nonlinear seepage.[31,32] Compared to water flooding, the injection pressure and start-up pressure of gas flooding are smaller. However, due to the low gas phase viscosity and relatively large gas−oil mobility ratio, gas is prone to viscous fingering in the reservoir, forming a dominant channel, and the problem of gas channeling is serious. This not only increases the amount of gas used but also significantly reduces crude oil recovery after breakthrough. With the continuous deepening of oilfield development, the reservoir environment becomes increasingly harsh and complex, and the chemical oil displacement agents used in conventional EOR technology have difficulty adapting to high temperature and salt reservoir conditions, further making it difficult to improve the oil washing efficiency.[33,34] Nanofluid flooding, as a new type of oil displacement technology for low permeability reservoirs, has attracted more and more attention due to its advantages, such as good injectability, small reservoir damage, strong oil displacement ability, and intelligent response.[35,36] This article developed a green biobased Janus nanomaterial, Bio-Nano30, through the self-assembly preparation method. This material has low interfacial free energy and can form a solid particle film with high interfacial strength, demonstrating excellent oil displacement performance. Through comparative experiments of water flooding and nanoagent flooding, the mechanism of the nanofluid reducing start-up pressure and improving oil displacement efficiency was elucidated.

2. EXPERIMENT

2.1. Experimental Study on Oil Displacement with Bio-Nano30. Based on the prepared Bio-Nano30 nanofluid (Bio-Nano30 is formulated using simulated formation water, interfacial tension of 0.1 wt % Bio-Nano30 is 10^{-3} mN/m), an indoor depressurization experiment was conducted. After injecting Bio-Nano30, the subsequent water drive pressure can be reduced by about 50% compared to that before injection, and the effect of reducing the displacement pressure is obvious. Bio-Nano30 is synthesized by supramolecular assembly method, and the reaction raw materials are nanosilica solid powder with median particle size of 50 and composite green biodegradable surfactant (the mass concentration ratio of nonionic surfactant and rhamnolipid biosurfactant is 1:1).

2.2. Experimental Parameters. Three artificial homogeneous sandstone cores with extremely low permeability were used for indoor simulated oil displacement experiments, with a core size of 2.5 × 2.5 × 10 (cm). The salinity of the formation in Daqing Oilfield is 4456 mg/L, and the simulated formation water is composed of distilled water according to Table 1.

3. DISCUSSION OF EXPERIMENTAL RESULTS

3.1. Interface Tension Test. As the concentration of Bio-Nano30 increases, the overall interfacial tension shows a decreasing trend (shown in Figure 1). Within a wide range of 0.1 to 0.6 wt %, the interfacial tension can reach an ultralow value of 10^{-3} mN/m.

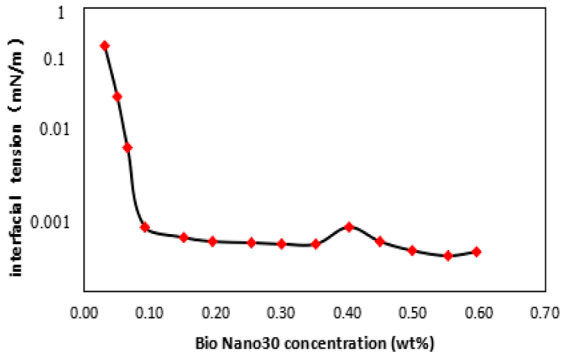

Figure 1. Effect of Bio-Nano30 concentration on interfacial tension.

3.2. Stability Test. Stability performance refers to the ability to maintain ultralow interfacial tension between injected Bio-Nano30 and crude oil (the experimental oil used is degassed paraffin-based crude oil from a third type reservoir in Daqing, with a wax content of 25.1%, a gum content of 15.7%, and an asphaltene content of 0.12%.) under formation conditions. Experimental data shows that the interfacial tension between oil and water remains within an ultra-low range under the action of the target nano agent. Therefore, the stability of Bio-Nano30 at a concentration of 0.1 wt % was studied. It was placed at a temperature of 45 °C and a mineralization degree of 4456 mg/L, and the interfacial tension was measured. With the extension of storage time, the interfacial tension between Bio-Nano30 and crude oil increases, maintaining an ultralow value within the measured 28 days (Table 2).

3.3. Nontoxicity Test Results. According to the environmental requirements, Bio-Nano30 has been tested. The sample may contain functional groups such as −OH, −NH, −COO−, −CON−, C = C, CH_2, CH_3 which was found by using infrared spectroscopy and nuclear magnetic resonance methods. It does not contain benzene ring substances, so it is impossible to contain OP (octylphenol) and NP (nonylphenol) surfactants.

3.4. Adsorption and Washing Resistance Achievement Test. In order to deepen our understanding of the mechanism of the depressurization injection of surfactants, we conducted experimental studies on the adsorption and flushing resistance of the surfactant system. A UV spectrophotometer was used to measure the absorbance of different surfactant systems at a certain wave length, by which a standard concentration curve can be drawn. This method is a fast and accurate means of testing the concentration of the surfactant

https://doi.org/10.1021/acsomega.3c02853
ACS Omega 2023, 8, 38926−38932

Table 2. Stability of the Bio-Nano30

time (d)	0	3	4	5	9	14	20	28
interfacial tension (10^{-3} mN/m)	2.39	3.01	2.13	2.50	6.76	2.98	6.64	8.75

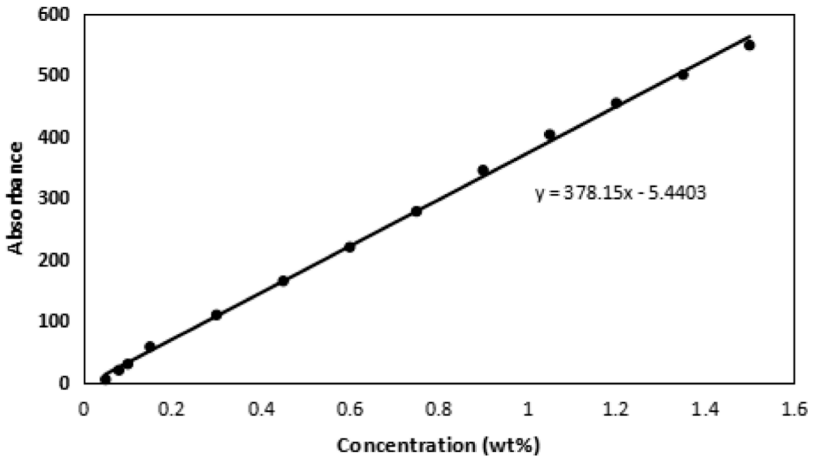

Figure 2. Standard curve of Bio-Nano30 concentration and absorbance.

Table 3. Experimental Program and Results

core number	Bio Nano30 concentration (wt %)	injection volume (PV)	injection Bio Nano30 (mg)	Bio Nano30 content in the produced liquid (mg)	adsorption capacity (mg)	adsorption capacity per unit pore volume (mg/mL)
D-1	0.1	0.3	1.5	1.279	0.221	0.044
D-2	0.1	0.5	2.6	2.358	0.242	0.048

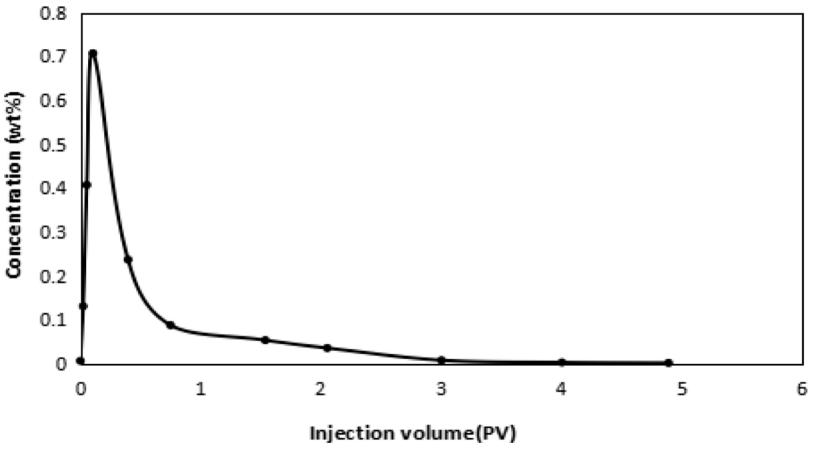

Figure 3. Variation of concentration in D-1 core outlet.

solutions. Figure 2 shows the absorbance concentration standard curve of the surfactant aqueous solution measured using a UV spectrophotometer.

3.5. Pressure Drop Test. Core depressurization experiments according to the water flooding Bio-Nano30 system was conducted followed by subsequent water flooding and the changes in the concentration of the surfactant system at the core outlet was measured (Table 3).

From Figures 3 and 4, it can be seen that the changes in the concentration and slug size led to the highest concentration of the surfactant system at the core outlet during subsequent water flooding processes, followed by a sharp decrease. After a sharp decrease in the concentration of the active agent at the core outlet, it remained at a lower concentration for about 5PV, and the active agent could not be detected at the core outlet. It indicates that a certain amount of active agent system

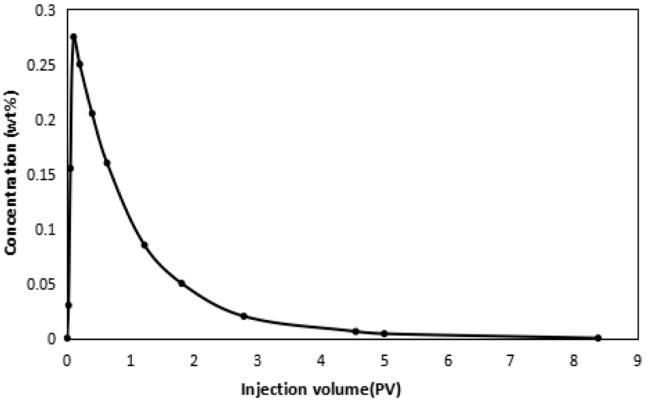

Figure 4. Variation of concentration in D-2 core outlet.

https://doi.org/10.1021/acsomega.3c02853
ACS Omega 2023, 8, 38926−38932

Table 4. Experiment Results of Oil Displacement

core	porosity (%)	permeability (10^{-3} μm^2)	original oil saturation (%)	water flooding			Bio Nano30		subsequent water flooding			pressure reduction value (%)	increased value of recovery rate (%)	EOR (%)
				PV	recovery ratio (%)	end pressure (MPa)	PV	recovery ratio (%)	PV	recovery ratio (%)	end pressure (MPa)			
E-1	22.3	28.6	77.0	2.44	40.3	2.30	0.16	1.81	1.21	10.58	1.24	45.9	12.39	52.69
E-2	22.6	30.2	74.0	2.20	41.3	2.25	0.19	1.25	0.90	10.70	1.11	50.6	11.95	53.25
E-3	22.2	31.6	74.7	2.57	42.7	2.41	0.12	0.70	1.22	10.84	1.27	47.5	11.54	54.24

Table 5. Laboratory Test Results of Displacement Pressure Decreased by Surfactant System

core number	porosity (%)	permeability (10^{-3} μm^2)	water flooding			Bio Nano30		pressure at the end of subsequent water flooding (MPa)	injection pressure ratio before and after pressure drop	pressure drop value (%)
			pore volume multiple	recovery ratio (%)	end pressure (MPa)	concentration (%)	interfacial tension (mN/m)			
B1	20.0	22.0	2.87	35.0	2.20	0.1	10^{-3}	1.45	1.98	50.5
B2	20.1	20.0	3.56	34.5	2.60	0.1		1.68	2.12	52.8
A1	11.6	3.2	2.68	27.5	1.20	0.1		1.63	1.64	39.2
A2	11.5	3.8	2.70	26.1	2.70	0.1		1.63	1.66	39.6

is adsorbed and retained in the pores of the core, and has not been displaced during subsequent water flooding processes. Therefore, this system can have a significant depressurization effect, and after being adsorbed on the surface of rock pores, it has a stronger flushing resistance.

3.6. Experimental Study on Oil Displacement. The oil displacement experiment method is as follows

① Permeability measurement of core model is measured.
② The experimental model is evacuated for 4 h, saturated formation water is injected into the model under vacuum conditions, and a constant temperature for 12 h at 45 °C is maintained.
③ Oil-driven water to bound water saturation is calculated.
④ Displacement water is injected into the model at a rate of 0.2 mL/min until no oil is produced at the model outlet. Bio-Nano30 with different injection volume at the same rate is injected, and then displacement water is injected until no oil is produced at the model outlet.

The experimental results are listed in Table 4. The increase in oil displacement efficiency is above 10%, and the injection amount is also relatively small, ranging from 0.12 to 0.19 PV.

As shown in Table 5, after injecting Bio-Nano30, the subsequent water flooding pressure can be reduced by about 50% compared to before injection, and the effect of reducing displacement pressure is obvious, especially for the ultralow permeability cores, which still has a good effect. As for core A1, the permeability is 3.8×10^{-3} μm^2, and after injecting 0.1 wt % Bio-Nano30, the pressure decreased by 39.6%; the permeability of core B1 is 20.0×10^{-3} μm^2, and after injecting 0.1 wt % Bio-Nano30 into m^2, the pressure decreased by 52.8%.

3.7. Analysis of Pressure Reduction Process Curve. Figure 5 shows the curve of displacement pressure versus the injected pore volume multiple during water flooding, Bio-Nano30 flooding, and subsequent water flooding. After water flooding to a certain pore volume, the displacement pressure is basically constant. At this time, after injecting 0.5 times the pore volume of the active agent system, and then subsequent water flooding, the pressure began to decrease significantly. After lowering to a certain value, it does not change until the end of the experiment. There is no rebound phenomenon. This indicates that the use of this active agent system can significantly reduce the displacement pressure of low-permeability cores, and cannot rebound in the subsequent water drive process.

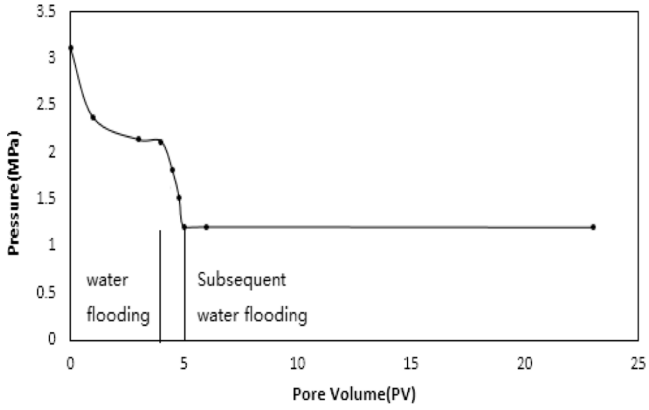

Figure 5. Pressure change of core (20×10^{-3} μm^2) in water flooding−surfactant flooding−succeeding water flooding.

According to the selected Bio-Nano30 oil displacement system (interfacial tension 10^{-3} mN/m), indoor pressure reduction experiments were conducted. It can be found that for low-permeability core models, the subsequent water drive pressure decreases by about 50% compared to before injection, and the effect of reducing displacement pressure is significant. The evaluation of ultralow permeability cores still shows good results. The main consideration is the Bio-Nano30 oil displacement system with ultralow interfacial tension, which changes the physical and chemical properties of the core wall during the injection process. The molecular layer adsorbed on the surface leads to a decrease in the capillary force resistance, resulting in a significant pressure drop effect.

3.8. Field Application. On the basis of indoor research, a single-well test was conducted to reduce pressure and increase injection according to the production needs of the L82−152-well in Daqing L Oilfield, China. The L82−152-well area is

https://doi.org/10.1021/acsomega.3c02853
ACS Omega 2023, 8, 38926−38932

located in the L522 block. The oil bearing area of this block is 12.42 km^2, with a geological reserve of 834.2 × 10^4 t. By adopting a reverse nine point area well network layout and synchronous water injection, there are a total of 149 oil and water wells, including 102 oil production wells, 85 open wells, 47 water injection wells, and 46 open wells. The average effective thickness of a single well is 10.5 m, the connecting thickness is 7.7 m, and the degree of water drive control is 73.2%. The initial injection pressure of the water injection well is below 10 MPa and can complete the injection water allocation. Due to the poor physical properties of the oil layer, the injection pressure quickly increases after injection, and the injection production pressure difference increases by an average of 1.57 MPa per year. The start-up pressure of water injection wells rises rapidly, with 46 wells injecting 1170 m^3 of water per day, with an average daily injection of 25 m^3 per well and a water injection intensity of 2.73 m^3/d·m. Among them, there are 23 wells with higher injection pressures, accounting for 50.0% of the number of wells opened. The average injection pressure is 15.5 MPa, with 735 m^3 of allocated injection and 591 m^3 of actual injection.

The water absorption capacity has also deteriorated year by year. The comparison of the water absorption profile data before and after the on-site single well test (Figure 6) shows

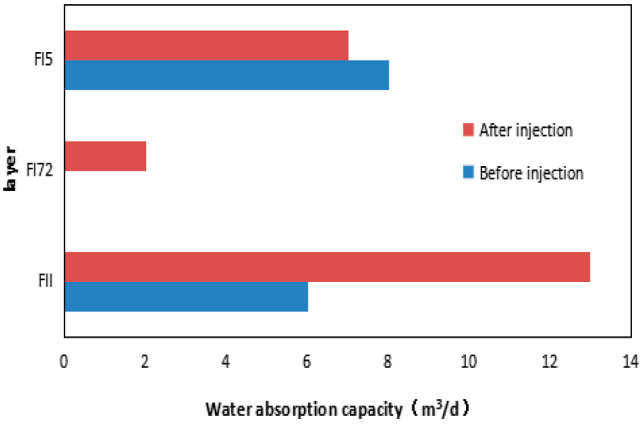

Figure 6. Intake capacity variation of each interval before and after surfactant system injection of a single well.

the water absorption thickness has increased by 2 m and the daily water injection rate increased from 14 to 22 m^3. Among them, the water absorption rate of the FI72 layer (2.0 m) increased from 0 to 2 m^3, and the daily water injection rate increased by 8 m^3, an increase of 57.1% compared to before the test. At an injection pressure of 15.3−15.9 MPa, the average daily injection volume was 19−22 m^3, respectively. Based on the current average daily injection volume of 21 m^3, the injection volume was increased by 50%.

3.9. Visualization Experiment for Oil Displacement.

Experimental conditions included transparent flat glass model of size 40 × 40 mm, oil wet. The experimental oil used was anhydrous degassed crude oil from the oil wells in the experimental area, which was mixed with kerosene to form a simulated oil with a viscosity of 9.8 mPa·s, and the experimental water was saline water with a salinity of 4456 mg/L. The experiment was conducted at room temperature and pressure. Oil displacement agent was 0.1 wt % Bio-Nano30.

As shown in Figures 7, 8 and 9, the large interfacial tension between crude oil and displacement fluid is the main factor

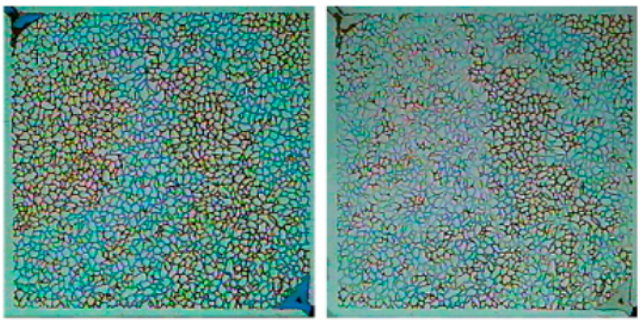

Figure 8. Comparative effects of oil displacement.

Figure 9. Wetting reversal before and after the action of Bio-Nano30 on the core (oil wet to water wet).

affecting the displacement effect. Due to the ultralow interfacial tension between Bio-Nano30 and crude oil, which increases the wetting contact angle of the oil phase, the wetting and adhesion tension of the crude oil are greatly reduced, resulting in a significant reduction in the adhesion work required for the oil to be pulled away from the rock surface. As a result, the oil washing ability of Bio-Nano30 is greatly improved, and the residual oil is driven to disperse into small oil droplets, while the large oil droplets in the large pores re-migrate, and move forward in gradual deformation. As the injection amount

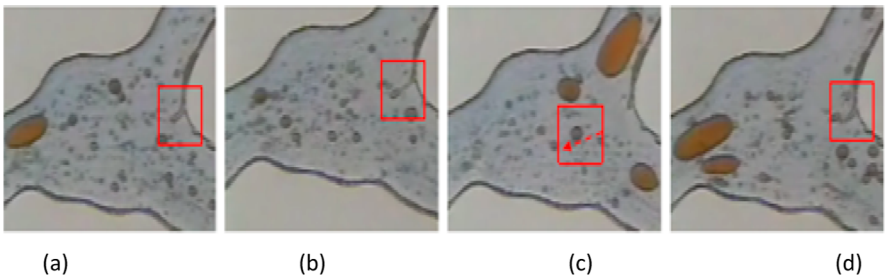

Figure 7. Dynamic diagram of crude oil in the reservoir affected by Bio. (a) Activation, protrusion, elongation of oil film (b) fracture and migration of oil filament (c) aggregation and migration of oil droplets, and(d) continued activation and migration of trapped oil.

https://doi.org/10.1021/acsomega.3c02853
ACS Omega 2023, 8, 38926−38932

increases, the residual oil that moves during the deformation process is pulled into slender oil threads that move forward. Due to the ability of Bio-Nano30 to emulsify crude oil and its water solubility, residual oil can form a large number of water in oil-emulsion-like small oil droplets during oil displacement. These emulsified small oil droplets are no longer easy to adhere to the rock surface and are carried by the oil displacement agent through the pore medium, improving oil displacement efficiency.

4. CONCLUSIONS

1. Bio-Nano30 can form ultralow interfacial tension with Daqing crude oil in the concentration range of 0.1−0.6 wt %. The interface activity "window" is relatively wide.
2. Under simulated geological conditions, Bio-Nano30 can still maintain ultralow interfacial tension values after being placed for 28 days.
3. Bio-Nano30 is green and environmental friendly; it does not contain benzene ring substances.
4. Bio-Nano30 has strong adaptability, interfacial activity, and stability in low permeability reservoirs.
5. Injecting a solution with a concentration of 0.1% into the core can reduce the injection pressure by 40−60% in indoor experiments, and the effect of reducing pressure and increasing injection is significant.
6. The results of single-well tests in the mine indicate that the thickness of water absorption in the oil layer increases, and the water absorption rate increases by 50%.

AUTHOR INFORMATION

Corresponding Authors

Jingchun Wu − *Key Laboratory for EOR Technology (Ministry of Education), Northeast Petroleum University, Daqing 163318, China*; Email: w6529@163.com

Fang Shi − *Key Laboratory for EOR Technology (Ministry of Education), Northeast Petroleum University, Daqing 163318, China*; orcid.org/0000-0002-4358-622X; Email: sfang1916@163.com

Authors

Yi Shen − *Key Laboratory for EOR Technology (Ministry of Education), Northeast Petroleum University, Daqing 163318, China*

Yingwei He − *Daqing Oil Field Company Limited, Daqing 163453, China*

Hongjun Li − *Daqing Oil Field Company Limited, Daqing 163453, China*

Wenxiu Zhou − *Daqing Oil Field Company Limited, Daqing 163453, China*

Manyong Zhao − *Daqing Oil Field Company Limited, Daqing 163453, China*

Chenying Wang − *Daqing Oil Field Company Limited, Daqing 163453, China*

Ying Yan − *Daqing Oil Field Company Limited, Daqing 163453, China*

Mingzheng Lu − *Daqing Oil Field Company Limited, Daqing 163453, China*

Jisheng Ma − *Daqing Oil Field Company Limited, Daqing 163453, China*

Lili Zheng − *Daqing Oil Field Company Limited, Daqing 163453, China*

Complete contact information is available at: https://pubs.acs.org/10.1021/acsomega.3c02853

Author Contributions

Y.S., J.W., and F.S. contributed equally to this work. F.S. contributed to formal analysis, funding acquisition, and resources. Y.S. contributed to data curation and Investigation. J.H. and J.W. contributed to methodology, and project administration. H.L., W.Z., M.Z., C.W., Y.Y., M.L., J.M., and L.Z. contributed to software. All authors have read and agreed to the published version of the manuscript.

Funding

Basic scientific research business expenses of Heilongjiang Provincial undergraduate universities guiding innovation fund of Northeast Petroleum University, Project number: 15071202205.

Funding

The data presented in this study are available in the article.

Notes

The authors declare no competing financial interest.

ACKNOWLEDGMENTS

Thank you for the equipment support provided by the Key Laboratory of Enhanced Oil and Gas Recovery, Ministry of Education.

REFERENCES

(1) Nourafkan, E.; Hu, Z.; Wen, D. Nanoparticle-enabled delivery of surfactants in porous media. *J. Colloid Interface Sci.* **2018**, *519*, 44−57.

(2) Liu, R.; Zhou, Q. X.; Ma, Q. Y. Applications of nanomaterials in remediation of contaminated water and soil: A review. *Chin. J. Ecol.* **2010**, *29*, 1852−1859.

(3) Zhao, M.; He, H.; Dai, C.; Sun, Y.; Fang, Y.; Liu, Y.; You, Q.; Zhao, G.; Wu, Y. Enhanced Oil Recovery Study of a New Mobility Control System on the Dynamic Imbibition in a Tight Oil Fracture Network Model. *Energy Fuels* **2018**, *32*, 2908−2915.

(4) Zhao, Y.; Yang, W.; Wang, D.; Wang, J.; Li, Z.; Hu, X.; King, S.; Rogers, S.; Lu, J. R.; Xu, H. Controlling the Diameters of Nanotubes Self-Assembled from Designed Peptide Bolaphiles. *Small* **2018**, *14*, 1703216.

(5) Luo, D.; Wang, F.; Zhu, J.; Cao, F.; Liu, Y.; Li, X.; Willson, R. C.; Yang, Z.; Chu, C.-W.; Ren, Z. Nanofluid of graphene-based amphiphilic Janus nanosheets for tertiary or enhanced oil recovery: High performance at low concentration. *Proc. Natl. Acad. Sci. U.S.A.* **2016**, *113*, 7711−7716.

(6) Zhang, Z.; Clarkson, C.; Williams-Kovacs, J. D.; Yuan, B.; Ghanizadeh, A. Rigorous Estimation of the Initial Conditions of Flowback Using a Coupled Hydraulic-Fracture/Dynamic-Drainage-Area Leakoff Model Constrained by Laboratory Geomechanical Data. *SPE J.* **2020**, *25* (06), 3051−3078.

(7) Liang, X.; Zhou, F.; Liang, T.; Su, H.; Yuan, S.; Li, Y. Impacts of pore structure and wettability on distribution of residual fossil hydrogen energy after imbibition. *Int. J. Hydrogen Energy* **2020**, *45* (29), 14779−14789.

(8) Pang, S.; Sharma, M. M. A Model for Predicting Injectivity Decline in Water Injection Wells. *SPE paper 28489 presented at 69th Annual Technical Conference and Exhibition held in New Orleans, LA*; OnePetro, 1994.

(9) Barkman, J. H.; Davidson, D. H. Measuring Water Quality and Predicting Well Impairment. *J. Pharm. Technol.* **1972**, *24*, 865−873.

(10) Nabzar, L.; Coste, J. P.; Chauveteau, G. Water Quality and Well Injectivity. *Paper 044, 9th European Symposium on Improved Oil Recovery*; European Association of Geoscientists & Engineers: Hague, The Netherlands, 1997.

(11) Eylander, J. G. R. Suspended Solids Specifications for Water Injection From Coreflood Tests. *SPE Reservoir Eng.* **1988**, *3*, 1287−1294.
(12) Vitthal, S.; Sharma, M. M.; Sepchrnoori, K. A One Dimensional Formation Damage Simulator for Damage due to Fines Migration. *Proc., SPE Symposium on Formation Damage Control*; SPE: Bakersfield, California, 1988; pp 29−42.
(13) Oort, E. v.; van Velzen, J. F. G.; Leerlooijer, K. Impairment by Suspended Solids invasion: Testing and Prediction. *SPE Prod. Facil.* **1993**, *8*, 178−184.
(14) Herzig, J. P.; Leclerc, D. M.; Goff, P. L. Flow of Suspensions through Porous Media-Application to Deep Filtration. *Ind. Eng. Chem.* **1970**, *62* (5), 8−35.
(15) Wennberg, K. I.; Sharma, M. M. Determination of the Filtration Coefficient and the Transition Time for Water Injection Wells. *SPE European Formation Damage Conference and Exhibition*; SPE, 1997; p 38181.
(16) Bedrikovetsky, P.; Marchesin, D.; Shecaira, F.; Souza, A. L.; Milanez, P.; Rezende, E. R. Characterisation of deep bed filtration system from laboratory pressure drop measurements. *J. Pet. Sci. Eng.* **2001**, *32* (2−4), 167−177.
(17) Bedrikovetsky, P.; Tran, T. K.; Van den Broek, W. M. G. T.; Marchesin, D.; Rezende, E.; Siqueira, A.; Souza, A. L.; Shecaira, F. S. Damage Characterization of Deep Bed Filtration from Pressure Measurements. *J. SPE* **2003**, *18* (02), 119−128.
(18) Amaefule, J. O.; Handy, L. L. The Effect of Interfacial Tensions on Relative Oil/Water Permeabilities of Consolidated Porous Media. *SPE J.* **1982**, *22*, 371−381.
(19) Leverett, M. C. Flow of Oil-Water Mixtures Through Unconsolidated Sands. *Trans., AIME* **1939**, *132*, 149−171.
(20) Mungan, N. Interfacial Effects in Immiscible Liquid-Liquid Displacement in Porous Media. *Soc. Pet. Eng. J.* **1966**, *6*, 247−253.
(21) Talash, A. W. Experimental and Calculated Relative Permeability Data for Systems Containing Tension Additives. *Paper SPE 5810 Presented at the SPE Improved Oil Recovery Symposium*; SPE: Tulsa, 1976.
(22) Gilliland, H. E.; Conley, F. R. Surfactant Waterflooding. *Proc., Ninth World Petroleum Congress, Tokyo*; WPC, 1975.
(23) Batycky, J. P.; McCaffery, F. G. Low Interfacial Tension Displacement Studies," paper 78.29.26 presented at the Petroleum Soc. of CIM. *29th Annual Technical Meeting*; PETSOC: Calgary, 1978.
(24) Bardon, C.; Longeron, D. Influence of Very Low Interfacial Tensions on Relative Permeability. *Soc. Pet. Eng. J.* **1980**, *20*, 391−401.
(25) Asar, H. Influence of Interfacial Tension on Gas-Oil Relative Permeability in a Gas-Condensate System. PhD Dissertation, U. of Southern California, Los Angeles, 1980.
(26) homas, C. P.; Winter, W. K.; Fleming, P. D., III Application of a General Multiphase, Multicomponent Chemical Flood Model to Temary, Two-Phase Surfactant Systems. *Paper SPE 6727 Presented at the SPE 52nd Annual Technical Conference and Exhibition*; SPE, 1977.
(27) Gupta, S. P.; Trushenski, S. P. Micellar Flooding-Compositional Effects on Oil Displacement. *Soc. Pet. Eng. J.* **1979**, *19*, 116−128.
(28) Pope, G. A. The Application of Fractional Flow Theory to Enhanced Oil Recovery. *Soc. Pet. Eng. J.* **1980**, *20*, 191−205.
(29) Wagner, D. R.; Leach, R. O. Effect of Interfacial Tension on Displacement Efficiency. *Soc. Pet. Eng. J.* **1966**, *6*, 335−344.
(30) Lefebvre du Prey, E. Influence des parameters interfaciaux sur les permeabilties relatives. *Comm. n°13, Comptes rendus du troisieme colloque de l'Association de Recherche sur les Techniques de Forage et de Production, Pau, France (Sept. 23−26, 1968)*; Editions Technip: Paris, 1969; pp 251−270.
(31) Gogarty, W. B.; Tosch, W. C. Miscible-Type Waterflooding: Oil Recovery with Micellar Solutions. *J. Pet. Technol.* **1968**, *20*, 1407−1414.
(32) Leverett, M. Flow of Oil-Water Mixtures Through Unconsolidated Sands. *Trans., AMIE* **1939**, *132*, 149−171.
(33) Moore, T. F.; Slobod, R. L. The Effect of Viscosity and Capillarity on the Displacement of Oil by Water. *Prod. Mon.* **1956**, *20* (10), 20.
(34) Taber, J. J. Dynamic and Static Forces Required To Remove a Discontinuous Oil Phase from Porous Media Containing Both Oil and Water. *Soc. Pet. Eng. J.* **1969**, *9*, 3−12.
(35) Cinar, Y. Effect of IFT Variation and Wettability on Three-Phase Relative Permeability. *SPE Reservoir Eval. Eng.* **2007**, *10*, 211.
(36) Dullien, F. A. L. *Porous Media-Fluid Transport and Pore Structure*, 2nd ed.; Academic Press: San Diego, 1992.

https://doi.org/10.1021/acsomega.3c02853
ACS Omega 2023, 8, 38926−38932